

Dry-gel conversion synthesis of SAPO-14 zeolites for selective conversion of methanol to propylene

Daizong Han ‡^a, Dongyuan Yang ‡^{c,d}, Chenyao Bi ^a, Guoqing Zhang ^a, Fei Yang ^a, Qingqing Hao^{a,b}, Jianbo Zhang ^{a,b}, Huiyong Chen ^{a,b,*}, Xiaoxun Ma^{a,b}

^a School of Chemical Engineering, Northwest University, Xi'an, Shaanxi 710069, China

^b International Science & Technology Cooperation Base for Clean Utilization of Hydrocarbon Resources, Chemical Engineering Research Center of the Ministry of Education for Advanced Use Technology of Shanbei Energy, Collaborative Innovation Center for Development of Energy and Chemical Industry in Northern Shaanxi, Northwest University, Xi'an, Shaanxi 710069, China

^c Shaanxi Key Laboratory of Energy Chemical Process Intensification, School of Chemical Engineering and Technology, Xi'an Jiaotong University, Xi'an, Shaanxi 710049, China

^d Shaanxi yanchang Petroleum (Group) Corp. Ltd., Xi'an, Shaanxi 710069, China

* Corresponding authors:

Prof. Huiyong Chen

Phone: (+86) 150 2993 2016

E-mail: hychen@nwu.edu.cn

‡ Daizong Han and Dongyuan Yang contributed equally to this work.

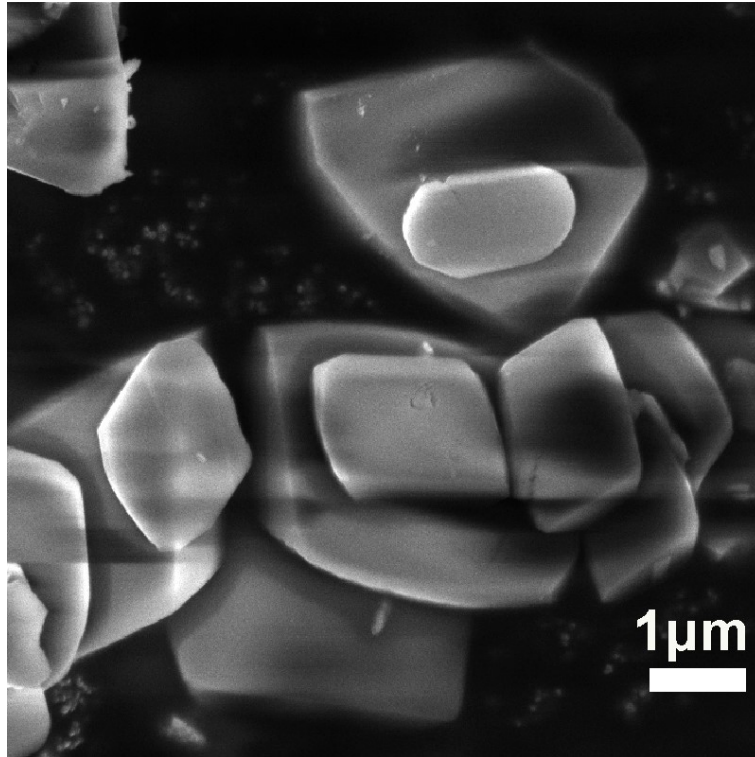


Figure S1. SEM image of SP14_HT.

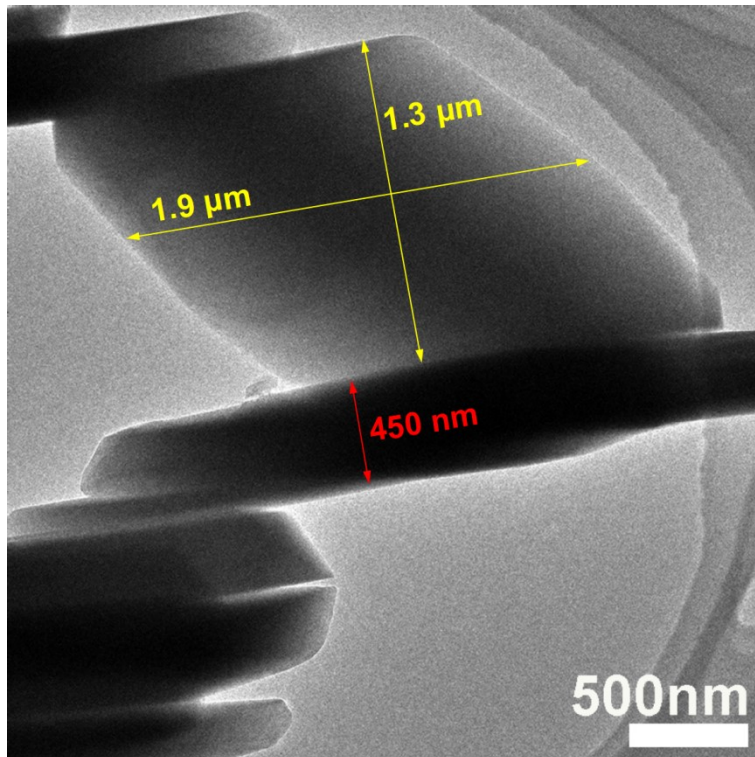


Figure S2. TEM image of SP14_DGC.

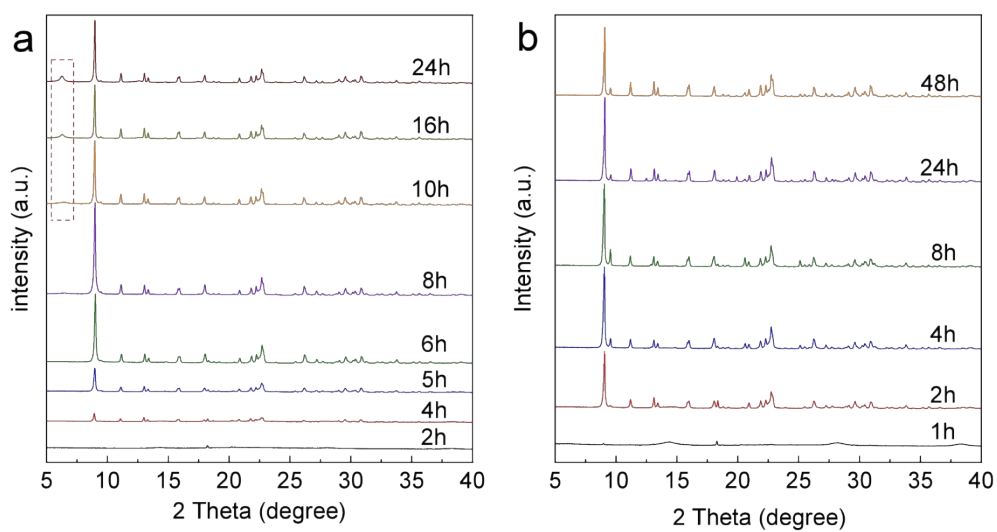


Figure S3. PXRD patterns of the SAPO-14 zeolites after different synthesis time by (a) dry-gel conversion and (b) hydrothermal treatment. (All the samples were fully washed by DI water and dried at 80 °C for 12 h.)

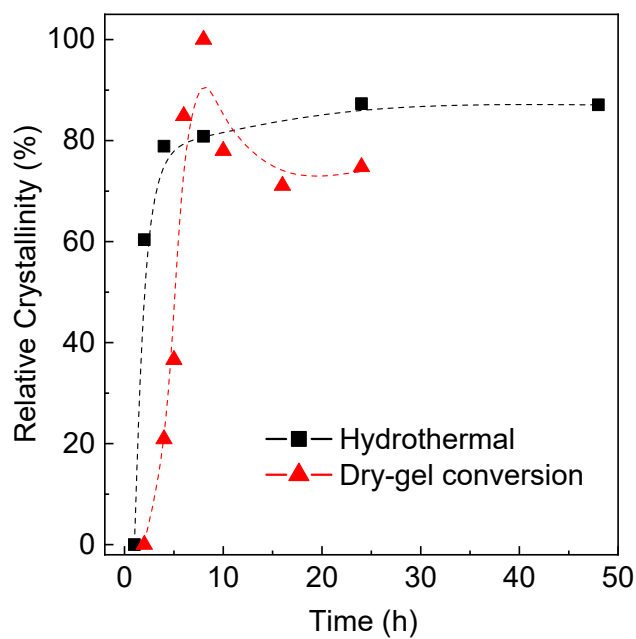


Figure S4. Crystallization curve over synthesis time by dry-gel conversion and hydrothermal treatment.

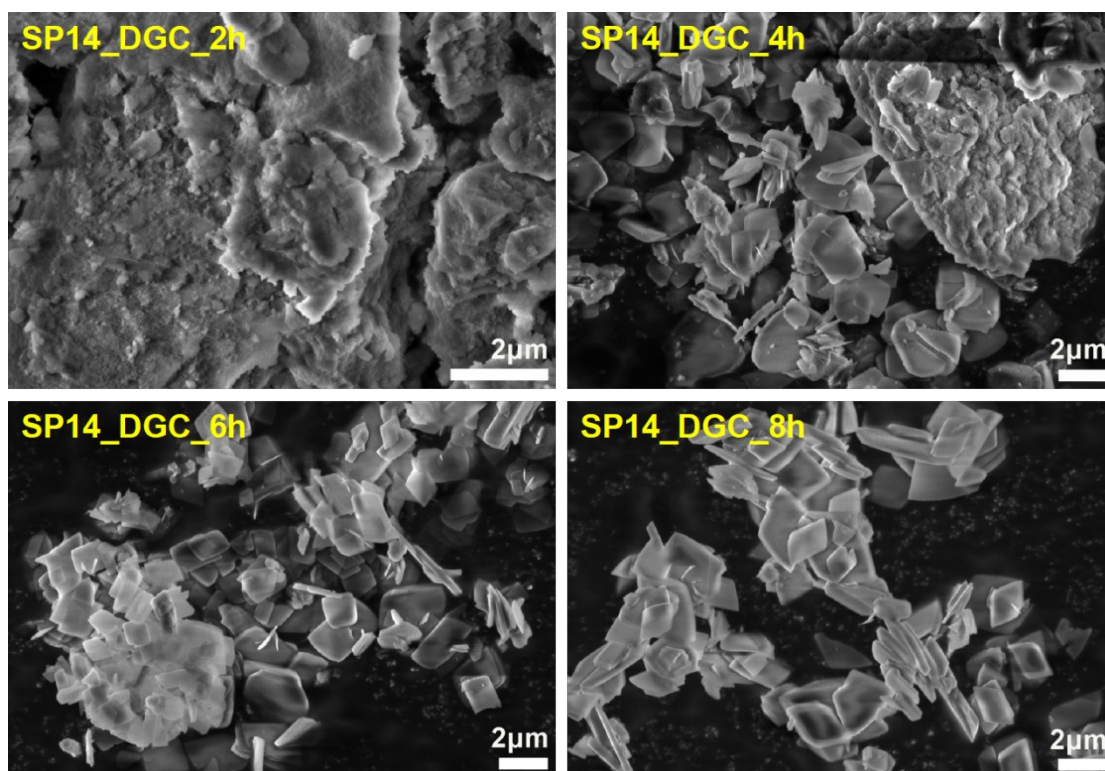


Figure S5. SEM images of the SP14_DGC samples after 2, 4, 6, and 8h of SAC treatments.

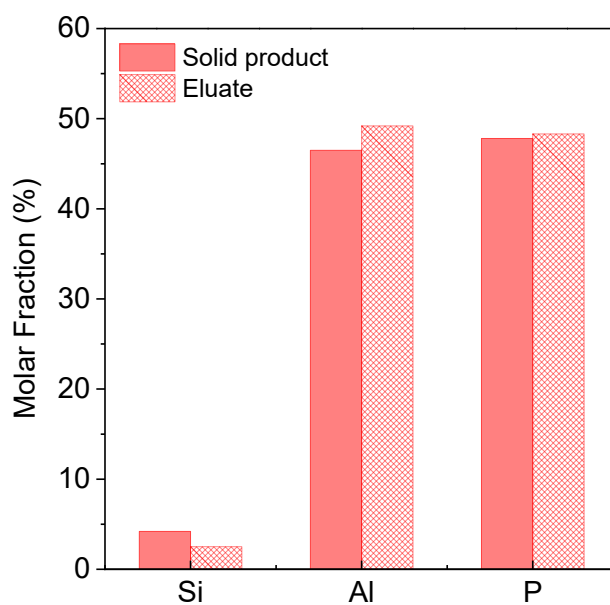


Figure S6. Molar fractions of Si, Al, and P in the solid product and eluate of SP14_DGC_8h.

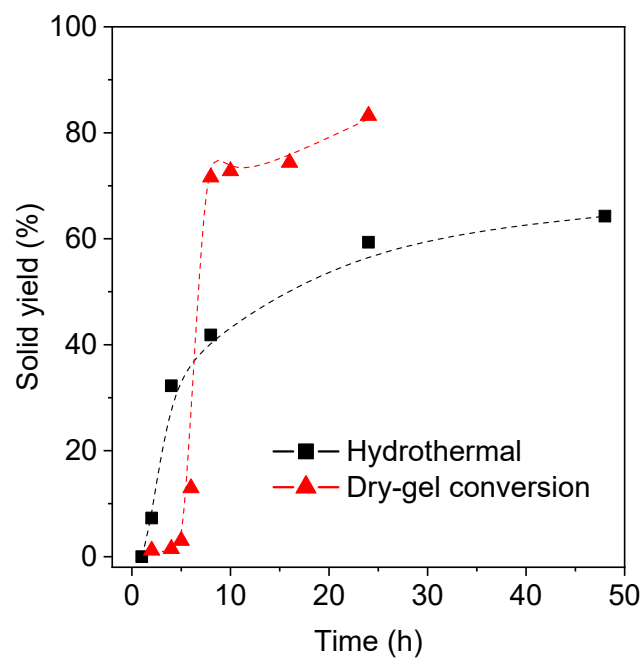


Figure S7. Product yields over synthesis time by dry-gel conversion and hydrothermal treatment.

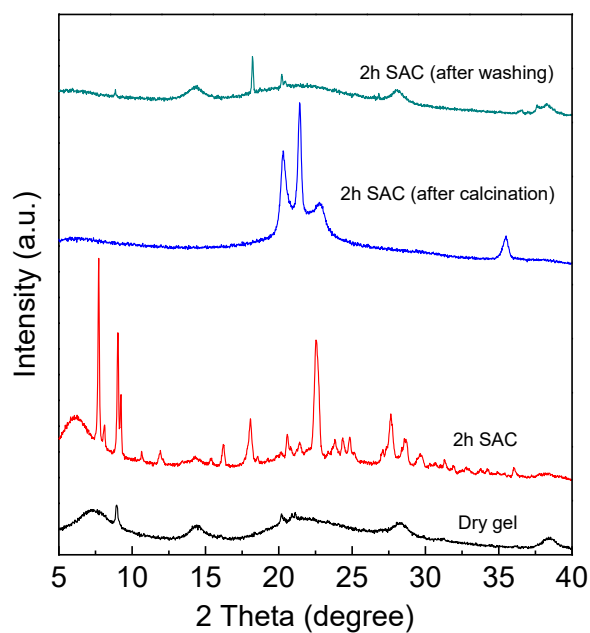


Figure S8. PXRD patterns of the synthesis dry gel and the sample after 2 h of SAC treatment. It was found that most of the crystalline aluminum and phosphorus

precursors were thermally unstable and could be destructed by calcination. On the other hand, the possible intermediate of silicate of EU-19 also transformed into silicon oxide. Moreover, all these species could be removed by simply washing, indicating their characteristic of solubility or dispersibility. It was believed that the stationary form of dry gel precursors could promote the phase transformation and the following nucleation of zeolites, which well explained the higher crystallization rate by dry-gel conversion than the conventionally hydrothermal synthesis.

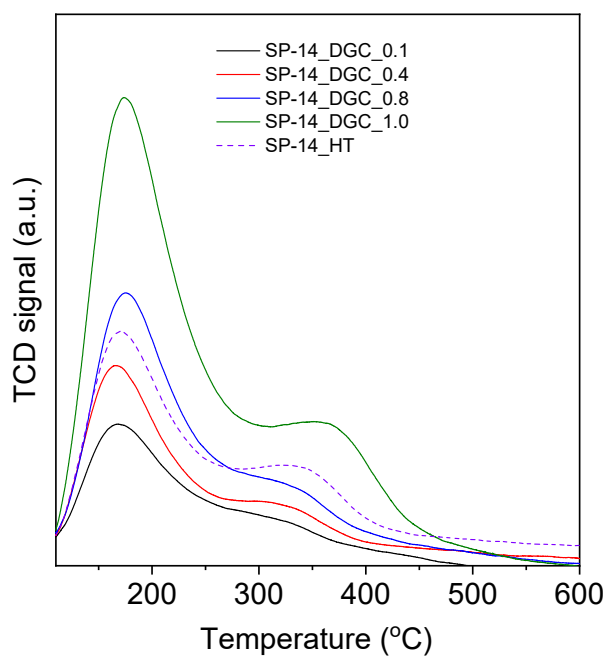


Figure S9. NH₃-TPD profiles of SP-14_HT and SP-14_DGC with various Si contents.

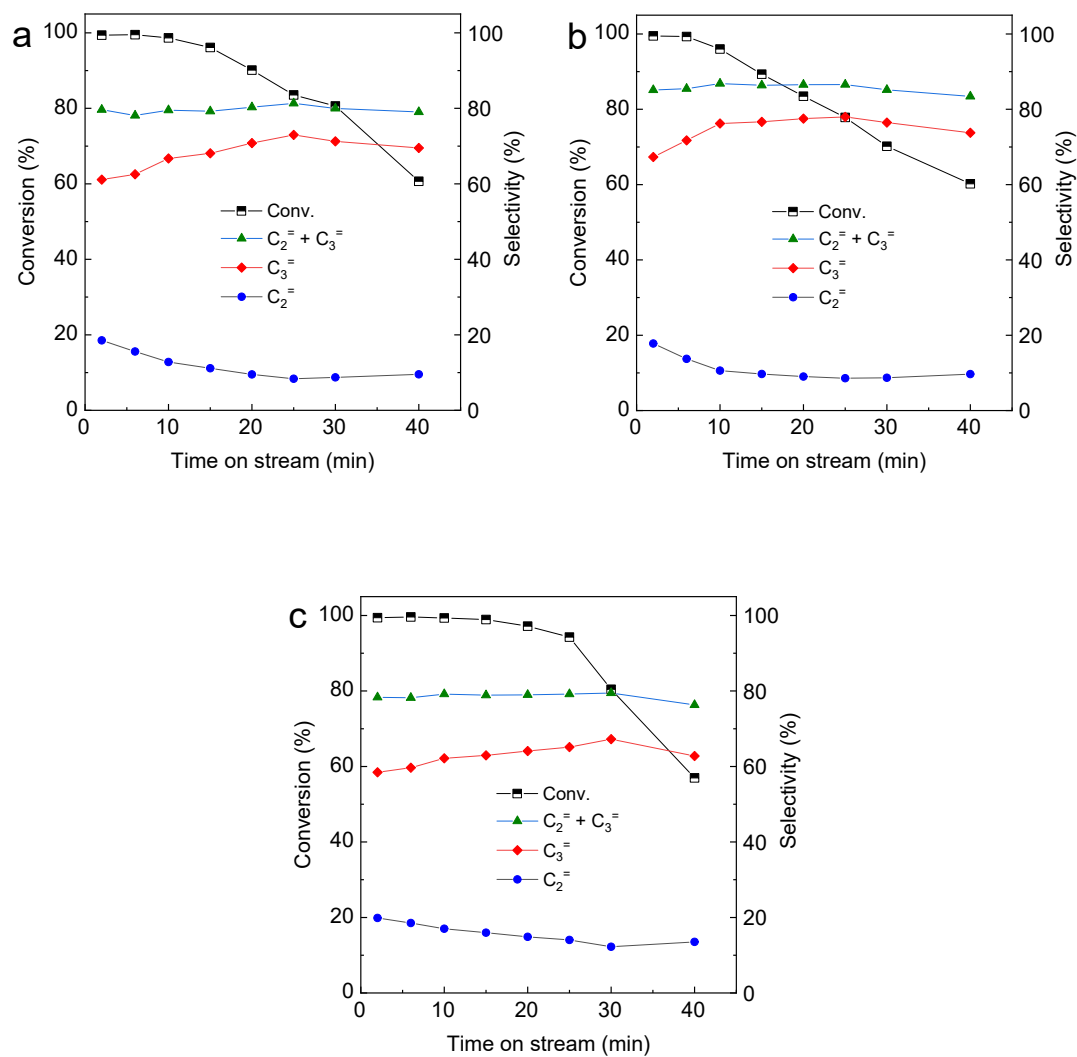


Figure S10. Methanol conversion and product selectivity over (a) SP-14_HT, (b) SP-14_DGC_0.8, and (c) SP-14_DGC_1.0.

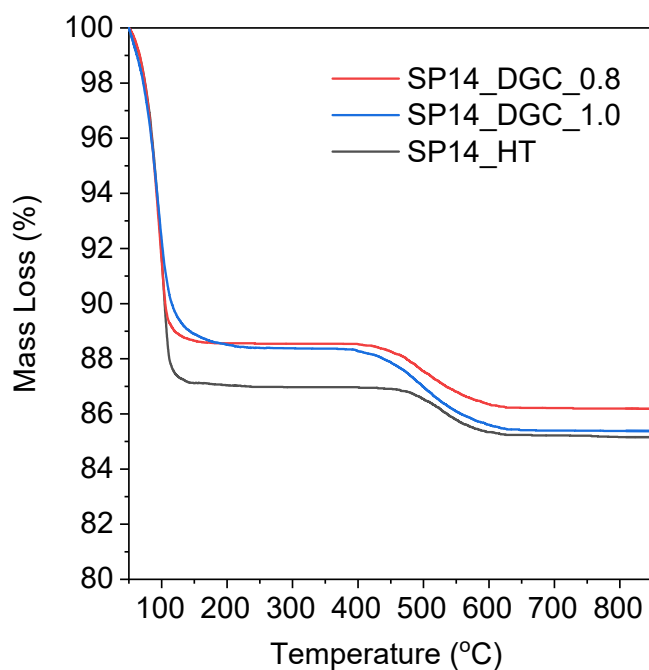


Figure S11. Weight losses of SP14_DGC_8.0, SP14_DGC_1.0, and SP14_HT catalysts after MTP reaction.

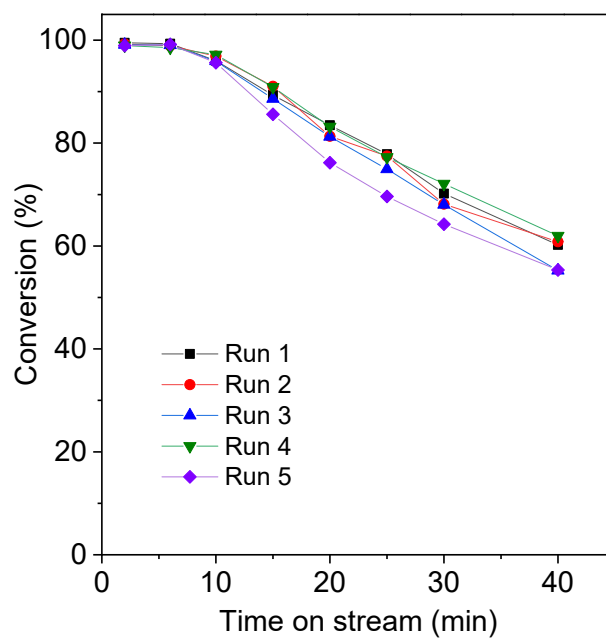


Figure S12. Methanol conversion over SP-14_DGC_0.8 in five runs of regeneration tests.

Table S1. Molar composition of the initial dry gel, mass ratio of water/gel, and crystalline phase of the corresponding products. (All the synthesis was proceeded at 180 °C for 8 h).

Molar composition of dry gel					Mass ratio of water/gel	Crystalline phase
SiO ₂	Al ₂ O ₃	P ₂ O ₅	SDA	H ₂ O		
0.00	1.00	1.00	3	2.27	4	AFN
0.10	1.00	1.00	3	2.27	4	AFN
0.40	1.00	1.00	3	2.27	4	AFN
0.80	1.00	1.00	3	2.27	4	AFN
1.00	1.00	1.00	3	2.27	4	AFN
1.00	0.50	1.00	3	2.27	4	AFN
0.00	1.00	0.50	3	2.27	4	AFN
0.00	1.00	0.33	3	2.27	4	AFN
0.33	1.00	0.33	3	2.27	4	AFN
1.50	1.00	1.00	3	2.27	4	AFN/CHA
2.00	1.00	1.00	3	2.27	4	CHA
1.00	2.00	1.00	3	2.27	4	CHA
0.00	1.00	0.10	3	2.27	4	Amorphous
3.00	1.00	1.00	3	2.27	4	Amorphous
0.50	1.00	0.10	3	2.27	4	Amorphous
1.00	0.10	1.00	3	2.27	4	Amorphous
1.00	1.00	0.10	3	2.27	4	Amorphous
0.00	0.50	1.00	3	2.27	4	Uncertain Structure
0.40	1.00	1.00	2	2.27	4	ATN
0.40	1.00	1.00	4	2.27	4	CHA
0.40	1.00	1.00	3	6.95	4	AFN
0.40	1.00	1.00	3	10.65	4	AFN
0.40	1.00	1.00	3	2.27	0.25	AFN
0.40	1.00	1.00	3	2.27	1	AFN

0.40	1.00	1.00	3	2.27	2	AFN
0.40	1.00	1.00	3	2.27	8	AFN
0.40	1.00	1.00	3	2.27	16	AFN
0.40	1.00	1.00	3	2.27	24	AFN

Table S2. Si content and acidity of various SP14_DGC catalysts and the contrast sample of SP14_HT synthesized by hydrothermal treatment.

Samples	Dry gel composition SiO ₂ /Al ₂ O ₃ /P ₂ O ₅ /i-PA/H ₂ O	Si content ^a (wt%)	Quantity of acid sites ^b (μ mol of NH ₃ /g, TPD)		
			Weak	Strong	Total
SP14_HT	0.1/1.0/1.0/3.0/50	0.73	0.18	0.08	0.26
SP14_DGC_0.1	0.1/1.0/1.0/3.0/2.27	0.31	0.09	0.02	0.11
SP14_DGC_0.4	0.4/1.0/1.0/3.0/2.27	0.68	0.12	0.04	0.17
SP14_DGC_0.8	0.8/1.0/1.0/3.0/2.27	0.75	0.20	0.06	0.26
SP14_DGC_1.0	1.0/1.0/1.0/3.0/2.27	0.87	0.37	0.18	0.54

^a Determined by ICP-OES;

^b Determined by NH₃-TPD and quantificationally calculated from the amounts of ammonia desorbed at 110–275 and 300–430 °C, respectively.

Table S3. Catalytic lifetime and product selectivity over SP14_HT and SP-14_DGC zeolites with various Si contents.

Samples	Lifetime ^a (min)	Product selectivity ^b (%)				P/E ^c
		C ₂ =	C ₃ =	C ₂ =+C ₃ =	C4-C6	
SP14_HT	15	12.8	66.7	79.5	14.0	5.22
SP14_DGC_0.1	-	20.1	59.1	79.2	17.0	2.93
SP14_DGC_0.4	-	18.4	63.6	82.1	12.5	3.45
SP14_DGC_0.8	10	10.6	76.2	86.8	9.6	7.19
SP14_DGC_1.0	20	17.0	62.2	79.2	14.4	3.66

^a Defined as the period with methanol conversion higher than 95% except for SP14_DGC_0.1 and

SP14_DGC_0.4, which manifested the highest conversion rate lower than 95%;

^b Taken at TOS = 10 min for SP14_HT, SP14_DGC_0.8, and SP14_DGC_1.0, and taken at the highest conversion for SP14_DGC_0.1 and SP14_DGC_0.4, respectively.

^c Defined as $S_{\text{propylene}}/S_{\text{ethylene}}$.